Theoretical and Spectroscopic Investigations of a Complex of Al(III) with Caffeic Acid

J. P. Cornard* and C. Lapouge

LASIR, CNRS UMR 8516, Université des Sciences et Technologies de Lille, Bât. C5, 59655 Villeneuve d'Ascq Cedex, France

Received: December 18, 2003; In Final Form: March 15, 2004

We investigate theoretically, by quantum DFT calculations, and by vibrational and electronic spectroscopies the complexation of Al(III) by caffeic acid. This compound presents two potential chelating sites in competition (catechol and carboxylic groups). In methanol solution, four different complexed species have been determined by spectrophotometry. The predominant species observed at low concentration of Al(III) has a 1:1 stoichiometry. The quantum chemical calculations show that the ligand involved in this complex undergoes small changes in electronic delocalization, compared with free caffeic acid. The structures of free and complexed ligands are slightly different. Calculations of vibrational transitions of caffeic acid and the 1:1 complex have permitted complete assignment of the experimental spectra. Modeling of electronic spectra in a vacuum and in methanol shows the necessity to take into account solvent effects in order to reproduce the experimental features. The assignments of UV−visible spectra of free and complexed ligands are very comparable, due to the similarity between the involved MOs in electronic transitions. The good accordance between theoretical and experimental data confirms that chelation of aluminum ion preferentially occurs at the deprotonated catechol site. This study illustrates that, in humic substances that include numerous polyphenolic and carboxylic functions in competition, the chelation does not involve the favored carboxylate group.

1. Introduction

Natural organic matter (NOM) is a heterogeneous mixture of compounds that does not have a uniform structural formula and possesses various potential metal binding sites. Humic substances that represent the main part of NOM are polyfunctional. These macromolecules may contain a large number of different complexing sites in competition, e.g., carboxylate, carbonyl, polyphenolic, or amine functional groups.[1] More than 40 types of binding sites in humic substances have been reported in the literature, as reviewed by Stevenson and Vance.[2] The study of soil organic matter−metal ion interactions is of considerable interest in soil science chemistry, and two general approaches could be envisaged for a better understanding of these interactions. One approach consists of studying the interactions in terms of general chemical and physical properties of the complexes formed with global NOM, but this kind of study reveals little about the structure of metal-binding sites. Another approach involves the study of complexing properties of model molecules which are representative of small, identifiable fractions of NOM. Numerous studies have shown that polyphenolic compounds, such as flavonoids, are non-negligible components of humic substances.[3−6] In previous works, we have focused our attention on complexation properties of a series of flavonoids toward Al(III).[7−11] Aluminum is described as a hard, trivalent ion, and, consequently, it can bind strongly to oxygen-donor ligands. We have compared the chelating power of different sites (hydroxycarbonyl and catechol), in competition within the same molecule, in methanol solution. We have shown that the complexing power of the different investigated groups could be classified in the order α-hydroxycarbonyl > β-hydroxycarbonyl > catechol, in neutral media.[12] As a continuation of this work, we now investigate the complexing properties of another polyphenol, the caffeic acid molecule, which possesses two coordination sites in competition, one at the catechol moiety and another at the carboxylic site. Caffeic acid, *trans*-3-(3,4-dihydroxyphenyl)propenoic acid, naturally occurs in many plants, together with other polyphenolic molecules. This phenolic compound plays an important role in soil chemistry, in relation with the formation of humic substances, and it participates in the transport of ionic metals present in the soil.[13]

Our main objectives were (i) to compare the chelating power of catechol and carboxylic groups, (ii) to determine the different complexed forms of caffeic acid with Al(III) in methanol and to identify the predominant species formed at low metal concentration, (iii) to achieve a structural analysis of caffeic acid and of its predominant complexed form by quantum chemical calculations, (iv) to obtain a complete assignment of vibrational and electronic spectra of caffeic acid and of its predominant complexed form, and (v) to situate the carboxylic group in the chelating power scale already obtained for other sites.

Our reasoning process was as follows. In a first step, the UV−visible spectra will allow us to determine the complexation mechanism of Al(III) by caffeic acid. From this mechanism, a hypothesis on the first implicated chelating site will then be proposed. The combined use of quantum chemical calculations and molecular spectroscopies will permit validation of our hypothesis and provide structural and spectroscopic features on caffeic acid and on its predominant complex formed for low Al(III) concentration.

2. Experimental Section

2.1. Reagents and Chemicals. The low solubility of caffeic acid in water prevents the acquisition of the high concentration necessary to record vibrational spectra in solution, so a methanolic solution was used. Caffeic acid was obtained com-

* Corresponding author. Tel.: + 33-3.20.43.69.26. Fax: + 33-3.20.43.67.55. E-mail address: cornard@univ-lille1.fr.

10.1021/jp0379188 CCC: $27.50
Published on Web 04/22/2004

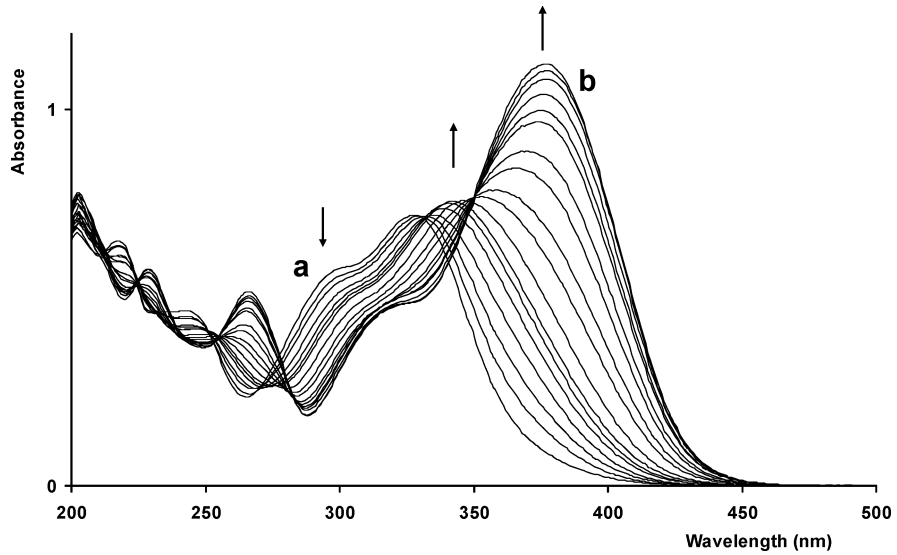

Figure 1. Electronic absorption spectra of caffeic acid in methanol in the absence and in the presence of $AlCl_3$. The molar ratios [Al(III)]/[CA] are, successively, from spectrum a to spectrum b: 0, 0.05, 0.07, 0.1, 0.13, 0.15, 0.17, 0.2, 0.25, 0.3, 0.4, 0.5, 0.7, 0.9, 1, 1.5, 2, and 5.

mercially from Sigma. Anhydrous aluminum chloride and spectroscopic grade methanol were used without purification.

The molar ratio method, introduced by Yoe and Jones,[14] has permitted the deduction of the composition of complexes in solution from spectrophotometric spectra. For this method, a solution containing a constant concentration (5×10^{-5} M) of caffeic acid in methanol and a variable concentration of $AlCl_3$ (from 10^{-6} to 2.5×10^{-4} M) was prepared. To verify the results obtained with the first method, the complexes' stoichiometries were also determined by the method of continuous variations (Job's method). The UV−visible spectra were recorded 24 h after the solution preparation in order to ensure that the equilibrium was reached. The solutions were stored in the dark to avoid photodegradation of the compounds.

2.2. Instrumentation. The UV−visible spectra were recorded on a Cary-1 (Varian) spectrophotometer with cells of 1 cm path length. FT-Raman spectra of caffeic acid and of its 1:1 complex with Al(III) in methanolic solution (10^{-2} M) and in solid form were recorded with a Bruker IFS 88W spectrometer connected to a Raman module (Bruker, FRA-106). Radiation of 1064 nm from a Nd:YAG laser was used for excitation with a laser power of 300 mW. An excitation in the near-infrared range allows the collection of fluorescence-free spectra. FT-IR spectra were recorded with a Bruker Vector 22 spectrometer operating with a resolution of 2 cm^{-1}. A concentration of approximately 2% in potassium bromide has been used both for the free ligand and for the 1:1 complex after a complete evaporation of solvent.

2.3. Calculations. The UV−visible spectra were refined using the Specfit software (version 3.0).[15] The set of spectra obtained at variable Al(III) concentrations were treated by evolving factor analysis (EFA)[16] in order to determine the number of absorbing species in the system and the pure electronic spectrum of each complex.

The DFT calculations were performed with the GAUSSIAN 98 quantum chemical package,[17] implemented on an IBM SP/Power 4 machine located at IDRIS (CNRS, France). Geometry optimizations, energy, and harmonic vibrational frequency calculations of caffeic acid and of its 1:1 complex were obtained by using the B3LYP hybrid functional[18,19] with the 6-31G** basis set, including polarization functions on all the atoms in order to correctly take into account the intramolecular H-bonding in free molecules. For the complex, water molecules have been added to the aluminum atom to obtain an octahedral environment of this ion and, thus, to maintain its valence. Computed vibrational frequencies were scaled by a factor of 0.972 for both the free ligand and the complex. This value corresponds to the average of the ratios of the experimental and calculated frequencies for each compound. Indeed, as scaling factors depend on the level of theory, the basis set, and the studied molecules,[20] we preferred to determine the best factor for our system, instead of using a predefined one. Bond orders of both compounds have been evaluated by the HONDO quantum mechanical package[21] from the Gaussian MOs.

The low-lying excited states were treated within the adiabatic approximation of time-dependent density functional theory (DFT-RPA)[22] with the B3LYP hybrid functional. Vertical excitation energies were computed for the first 30 excited states to reproduce the UV−visible spectra of free and complexed molecules. Solvent effects on calculated UV−visible spectra were introduced by the SCRF method, via the Self-Consistent Isodensity Polarized Continuum Model (SCIPCM)[23] implemented in the Gaussian program. In our results, only transitions presenting high oscillator strengths have been considered, without focusing on their relative values, because it is well known that, in such calculations, relative oscillator strengths are not reliable.

3. Results and Discussion

3.1. Stoichiometry of Complexes in Methanol. The electronic spectrum of free caffeic acid in methanolic solution (Figure 1, spectrum a) is mainly characterized by an important absorption double band at 317 and 294 nm and a band located at 215 nm, with a shoulder at 237 nm. The addition of anhydrous $AlCl_3$ to the caffeic acid (CA) solution in methanol results in important spectral modifications, with the apparition of a new band at higher wavelengths. For [Al(III)]/[CA] ratios less than 1, the set of obtained spectra shows that this new band shifts toward the long wavelengths in accordance with the amount of $AlCl_3$ added. That no isobestic point is observed for these ratios seems to indicate the simultaneous presence of several complexed species in solution. For [Al(III)]/[CA] ratios greater than 1, an isobestic point is obtained at 350 nm, indicating an equilibrium between two species. For large amounts of Al(III) added ([Al(III)]/[CA] $\geq$ 5), one observes the final complex spectrum ($\lambda_{max} = 377$ nm).

The molar ratio method was used to determine the stoichiometry of the different complexed forms of caffeic acid with aluminum(III). The molar ratio plots at different wavelengths (317, 342, and 377 nm) clearly show the presence of four species of stoichiometry Al(III):CA = 1:6, 1:3, 1:1, and 2:1. The application of the continual variations method (Job's method) to our set of data gives rise to the same results. The treatment of UV−visible spectra, obtained at variable Al(III) concentration, by evolving factor analysis (Spectfit program) shows five absorbing species, including the free ligand. In the first step of the dosage, at low concentrations of $AlCl_3$, one observes the simultaneous formation of the three complexes 1:6, 1:3, and 1:1. The predominant form is obviously the 1:1 complexed species. The 1:6 complex occurs in very low concentration and merely appears for extremely small [Al(III)]/[CA] ratios. In these three complexed forms, one can suppose that only one complexing site is occupied by one Al(III) entity. If anhydrous aluminum chloride has a dimeric form (Al_2Cl_6) in the solid state, this dimer is broken before or during the complexation process, as no binuclear complex is observed for [Al(III)]/[CA] ratios less than 1. For [Al(III)]/[CA] ratios greater than 1, the presence of the isobestic point, observed at 350 nm, shows that the complexation of the first site is completed (complex 1:1), and, therefore, the second chelating site begins to coordinate Al(III), leading to the formation of the 2:1 complex. This mechanism seems to show that the chelating power is very different for the two sites in competition. Indeed, the weaker site should be engaged only after the stronger one is fully occupied.

Two works concerning the behavior of caffeic acid toward aluminum ions in aqueous solution have already been published. Sikora and McBride[24] report the formation of only one complex of 1:1 stoichiometry in solution at pH = 4.6. They also observe a variation of the shape of the absorption band assigned to a modification of the protonation state of the ligand with pH. This is in contradiction with a more recent article published by Adams et al.,[25] which describes a system that simultaneously presents the 1:1, 1:2, and 1:3 species with different concentrations as a function of pH. These authors also report the stability constant of each complexed form obtained from potentiometric titrations. However, they do not find simultaneous coordination of metal ions to both sites, but the upper limit of the metal-to-ligand ratio (less than 1) used in their work was insufficient to form the 2:1 complex in water. The conclusion of their works is that whatever the pH, even for pH = 3, Al(III) is coordinated to the doubly deprotonated catechol site. For pH = 4, the predominant species is $AlHL^+$, whereas, for pH = 5, AlL^0 predominates (where H_3L denotes caffeic acid). A pH increase gives rise to the preponderance of the 1:2 and 1:3 complexes with totally deprotonated ligands. One can notice that the formation of AlL_2^{3-} occurs at pH = 5, and becomes preponderant at pH = 6.5. Similarly, AlL_3^{6-} species begin to appear at pH = 6.5. Thus, even in acidic media, complexes of high stoichiometry can be observed.

It is well known that the catechol group is a powerful complexing agent for Al(III), and, despite its extremely high pK_a values, this function is able to coordinate Al(III) at very low pH with a complete deprotonation of the hydroxyl groups. The presence of a chelate obtained with a protonated catechol group has never been observed in water.[26−29] Other studies[8,30,31] concerning the chelation in methanol solution of Al(III) by polyphenols (flavonoids family), which present the catechol group, lead to the same conclusions as those obtained in water. Complexes of 1:1, 1:2, and 1:3 stoichiometry are formed through the catechol function presenting deprotonated hydroxyl groups.

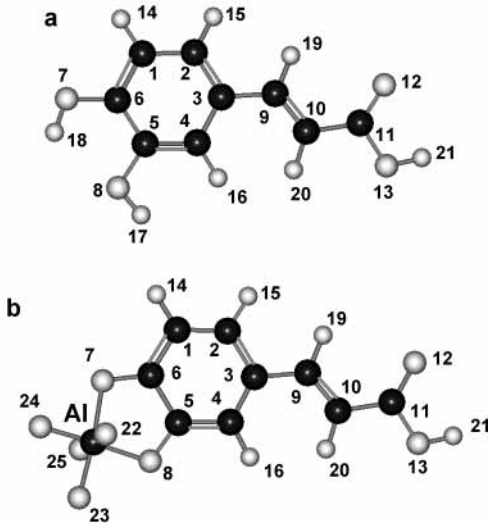

Figure 2. Numbering scheme used in the text for (a) caffeic acid and (b) its 1:1 complex (only the oxygen atoms of water molecules are shown).

From our experimental results and those found in the literature, we can issue the hypothesis that the complexation of Al(III) in a methanol solution of caffeic acid occurs with the catechol group for mononuclear species. In these complexes, the two OH ring groups are supposedly deprotonated. In opposition, the carboxylic group must be mainly protonated, because the complexation reaction occurs in a medium containing only acidic species. In these conditions, the formation of the 1:6 complex, at very low concentrations of Al(III), could be explained by the coordination of three caffeic acid dimers to an aluminum ion, the dimerization of caffeic acid taking place through the carboxylic acid group. At a large excess of Al(III), all catechol sites must be engaged in complexation, at which time, an aluminum entity would be able to coordinate the carboxylate function, giving rise to the 2:1 chelates. Some reported results concerning the complexation of copper(II) and iron(II) clearly show the ambidentate nature of caffeic acid.[32−34] Hence, besides chelation via the catechol site, the carboxyl group can also take part in the coordination by forming monomeric or oligomeric complexes in which both binding sites of the ligand are involved in the coordination.

Both in water (literature) and in methanol (this study), the 1:1 complex, deprotonated on catechol and protonated on the carboxylate group, has been observed either by potentiometric titration or by electronic spectroscopy. However, although these two analytical techniques are very sensitive, they do not allow for acquiring the necessary information to unambiguously determine the molecular structure of the compounds. That is the reason we have performed a vibrational analysis of this complex in order to characterize its molecular structure and to confirm our hypothesis.

3.2. Conformational Analysis. A complete conformational analysis of caffeic acid at the DFT level has been recently published.[35] This article describes the different stable conformers of the molecule. For all our calculations concerning caffeic acid, we started from the most stable conformer geometry previously found, which presents a planar structure and a medium strength intramolecular H-bond between O8 and H18 in the catechol group (Figure 2a). A complete geometry optimization was carried out for the 1:1 complex, considering a coordination of aluminum(III) at the doubly deprotonated catechol site. Four water molecules were added to take the aluminum valence into account, leading to the formula $[Al(CA)(H_2O)_4]^+$. The atom

TABLE 1: Calculated Geometrical Parameters of Caffeic Acid and of Its 1:1 Complex: Bond Lengths (Å), Angles (°), and Main Dihedral Angles (°)

bond lengths			bond angles		
	caffeic acid	complex		caffeic acid	complex
C1C2	1.393	1.397	C3C4H16	120.3	121.2
C2C3	1.405	1.406	C4C5O8	124.9	123.8
C3C4	1.413	1.413	C5O8H17	110.1	
C4C5	1.383	1.384	C5C6O7	120.3	116.0
C5C6	1.411	1.419	C6O7H18	107.8	
C6C1	1.392	1.389	C3C9H19	115.8	116.0
C3C9	1.456	1.462	C9C10H20	123.3	123.5
C9C10	1.348	1.345	C10C11O12	126.6	125.9
C10C11	1.470	1.477	C10C11O13	111.5	111.3
C6O7	1.357	1.382	O12C11O13	121.9	122.7
C5O8	1.375	1.379	C11O13H21	105.6	106.1
C11O12	1.218	1.215	C5O8Al		107.3
C11O13	1.362	1.357	C6O7Al		106.6
C1H14	1.085	1.085	O7AlO22		88.0
C2H15	1.086	1.086	O7AlO23		96.6
C4H16	1.087	1.085	O7AlO24		178.1
O8H17	0.965		O7AlO25		88.8
O7H18	0.970				
C9H19	1.089	1.089	C1C2C3C4	0.0	0.0
C10H20	1.085	1.085	C2C3C4C5	0.0	0.0
O13H21	0.972	0.972	C3C4C5C6	0.0	0.0
O7Al		1.792	C4C5C6C1	0.0	0.0
O8Al		1.778	C1C2C3C9	180.0	179.9
AlO22		2.037	C2C3C9C10	180.0	179.8
AlO23		1.992	C3C9C10C11	180.0	179.9
AlO24		1.968	C3C4C5O8	180.0	180.0
AlO25		2.026	C4C5C6O7	180.0	179.9
			C4C5O8H17	0.0	
C1C2C3	121.5	121.7	C5C6O7H18	0.0	
C2C3C4	118.1	118.8	C2C3C9H19	0.0	0.1
C3C4C5	120.5	119.9	C3C9C10H20	0.0	0.0
C4C5C6	120.7	120.6	C9C10C11O12	0.0	0.0
C5C6C1	119.3	120.1	C9C10C11O13	180.0	180.0
C2C3C9	118.9	118.5	C10C11O13H21	180.0	180.0
C3C9C10	128.2	127.9	C6O7AlO22		98.1
C9C10C11	120.0	119.7	C6O7AlO23		179.6
C6C1H14	118.6	119.8	C6O7AlO24		47.1
C1C2H15	119.4	119.3	C6O7AlO25		98.6

TABLE 2: Calculated Bond Orders of Caffeic Acid and Its 1:1 Complex

	caffeic acid	complex		caffeic acid	complex
C1C2	1.42	1.41	C10C11	1.05	1.03
C2C3	1.44	1.44	C6O7	0.91	0.78
C3C4	1.37	1.37	C5O8	0.83	0.77
C4C5	1.48	1.50	C11O12	1.78	1.80
C5C6	1.32	1.30	C11O13	0.97	0.98
C6C1	1.45	1.47	O7Al		0.74
C3C9	1.07	1.05	O8Al		0.77
C9C10	1.79	1.82			

numbering of caffeic acid and the 1:1 complex used in this paper is reported in Figure 2. The most relevant structural parameters, bond lengths, valence, and dihedral angles of caffeic acid and of its 1:1 complex determined with B3LYP/6-31G** method are given in Table 1. The comparison of the parameters of the free and complexed ligands does not show important structural changes. The benzene ring structure is very slightly modified; a small increase of the C5−C6 bond length is observed in the complex, due to the coordination to aluminum ion inducing a more important steric hindrance. Due to the presence of the intramolecular H-bonding, the two C−O bond lengths of the catechol group are very different in the free molecule. In the complex, a marked increase of the C6−O7 bond length is calculated, and the two C−O bonds are almost identical. At the chelating site, the Al−O bond lengths involving the oxygen atoms of the catecholate group are calculated to be shorter than those involving the oxygen atoms of water molecules. A pronounced decrease of the C4−C5−O8 and C5−C6−O7 valence angles is observed in the complexed form. The electronic delocalization along the chain is slightly reduced in the complex, with respect to the free ligand. Indeed, an increase of C3−C9 and C10−C11, accompanied by a decrease of C9−C10 and C11−O12 bond lengths, is observed. However, the aliphatic carbon structure remains coplanar with the aromatic ring; only very low variations of dihedral angles have been calculated for the complexed ligand, compared to the free molecule. The calculation of bond orders confirms all these observations (Table 2). On the free molecule, one can notice that electronic delocalization is not regular; indeed, the intramolecular H-bond is responsible for a considerable decrease of the C5−C6 bond order and an increase of the order of adjacent bonds. This effect is emphasized in complex formation, where the bond order of C5−C6 falls to 1.30. A reduction of the electronic delocalization along the aliphatic part of the complex is also confirmed by the bond-order calculation, showing that values of 1.82 and 1.80 are reached for the C9−C10 and C11−O12 bond orders. To evaluate the solvent effects on structure for the two studied compounds, their geometries were optimized in methanol with the SCRF method by the Poisson−Boltzmann solver[36,37] implemented in the Jaguar package.[38] This program has been chosen for its efficiency and rapidity for such calculations. The geometrical parameters calculated with this method differ very slightly from those obtained in a vacuum, and are, thus, not reported in this paper. Nevertheless, even if solvent effects are negligible from a conformational point of view, such is not the case for the electronic properties, as we will see in the UV−visible spectra calculation.

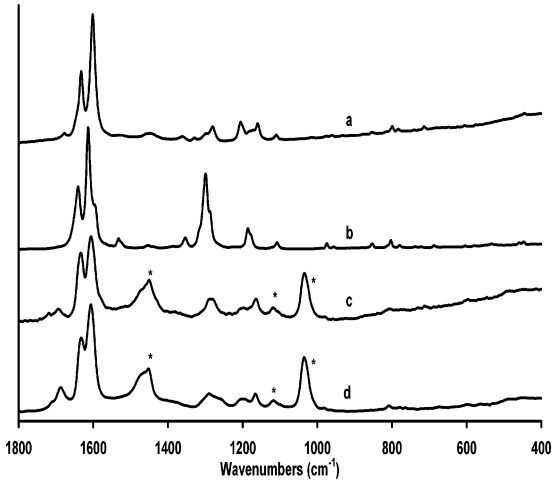

Figure 3. FT-Raman spectra of (a) the 1:1 complex in the solid state, (b) caffeic acid in the solid state, (c) the 1:1 complex in solution, and (d) caffeic acid in solution. The asterisks indicate solvent bands.

3.3. Vibrational Spectroscopy. Although FT-Raman or surface-enhanced Raman spectra of caffeic acid have been recently published,[39−41] a complete assignment of the vibrational spectra has not been found in the literature. Some articles mentioning the infrared spectroscopy of this compound are limited to a discussion on the C═O band of the carboxylic function. Here, we have established a total assignment of vibrational spectra of caffeic acid and of its 1:1 complex with the help of harmonic vibrational frequency calculations. The FT-Raman spectra, in the range 400−1800 cm^{-1}, of the free and complexed ligand in the solid state and in methanol solution are presented in Figure 3. The FTIR spectra reported in Figure 4 relate to the solid state (KBr pellets). To be sure that only the

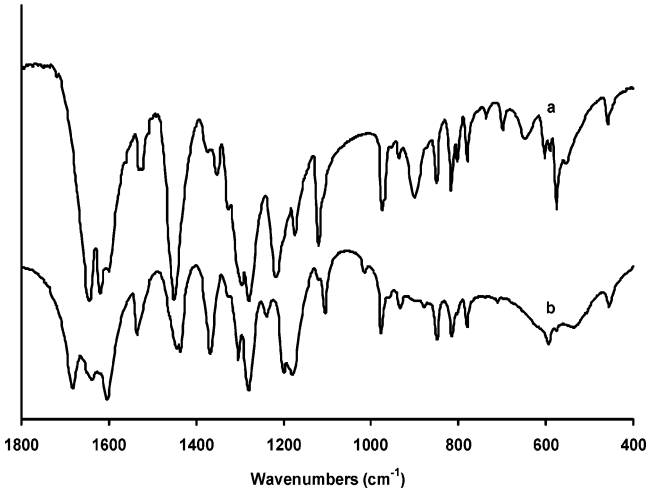

Figure 4. FTIR spectra of (a) caffeic acid and (b) its 1:1 complex in the solid state.

complex of 1:1 stoichiometry was present in solution, an [Al(III)]/[CA] ratio of 1 has been used; for this value, the predominant species is unambiguously the 1:1 complex. The complex in the solid state, in powder form, was obtained by evaporation of methanol under vacuum.

The FTIR and FT-Raman spectra recorded on the solid-state molecules show relatively major differences between the free and complexed forms of caffeic acid, whereas the shapes of the Raman spectra are similar for caffeic acid and the 1:1 complex in solution. The calculated and observed wavenumbers, as well as the vibrational assignment, are given in Tables 3 and 4 for caffeic acid and the 1:1 complex, respectively. The computed frequencies were scaled by an empirical factor to reproduce, as widely as possible, the experimental values. Wilson's notation[42] was used to describe the characteristic benzene ring vibrations involved in the different normal modes.

The C═O stretching of the carboxyl group in the free ligand is observed only in solution at 1687 cm^{-1}, in total disagreement with Williams et al.[43] who assigned this vibrational mode to the infrared band located at 1644 cm^{-1}. On the other hand, this stretching mode appears both in solution (1693 cm^{-1}) and in solid-state Raman (1677 cm^{-1}) and IR (1684 cm^{-1}) spectra for the complex. These wavenumber shifts of this mode in the complex could easily be explained by an increase of intermolecular hydrogen bonding in the different sample forms. Indeed, the number and the strength of hydrogen bonds decrease when going from pure crystalline powder (Raman), to dispersed compound in KBr (infrared), to solution (Raman). A small increase of the C═O stretching frequency is observed in solution for the complexed form (1693 cm^{-1}), with respect to the free ligand (1687 cm^{-1}). This trend is in agreement with the augmentation of the bond orders calculated to 1.78 and 1.80 for the free and complexed ligands, respectively. However, one can note that this very small modification in frequency confirms

TABLE 3: Calculated (Scaled by 0.972) and Experimental Vibrational Frequencies of Caffeic Acid and Tentative Assignment According to Wilson's Notation for Benzene Rings[a]

	experimental			
calculated	infrared (solid)	Raman (solid)	Raman (solution)	tentative assignment
1760			1687	ν(C11O12)
1648	1645	1641	1635	ν(C9C10) + 8b
1616	1619	1614		8b + ν(C9C10)
1602	1601	1597	1606	8a + δ(C6O7H18)
1529	1529	1531		19a + δ(C5O8H17)
1452	1450	1454		19b
1394	1376			δ(C6O7H18)
1359	1352	1354		δ(C11O13H21) + δ(C6O7H18) + δ(C9C10H20)
1329	1327			14 + δ(C3C9H19)
1309	1312	1316		14 + δ(C3C9H19)
1290	1296	1299	1290	7a + ν(C6O7) + δ(C11O13H21)
1264	1280	1287		14 + νas(C6O7,C5O8) + δ(C11O13H21)
1236	1212	1223		3 + δ(C9C10H20) + δ(C11O13H21)
1186	1199	1186	1196	14 + δ(C6O7H18)
1160	1174	1178	1166	18b + ν(C3C9)
1141				18a + ν(C3C9) + ν(C5O8) + δ(C5O8H17)
1120	1120	1125		18a + ν(C3C9) + ν(C11O13) + δ(C11O13H21)
1103	1106	1108		18a + ν(C5O8) + δ(C5O8H17)
1003	975	974		γ(C9H19) + γ(C10H20)
967	953	957		18b + δ(C3C9C10C11)
940	935			18b + ν(C10C11) + ν(C11C12)
916	901			17b
853	850	853		11 + γ(C10H20)
820				11
794	817	811	808	12
805	802	803		5 + γ(C9C10C11)
755	780	780		12 + δ(C3C9C10)
729	737	738		4 + γ(O13H21)
674	699	687		4 + γ(O13H21) + δ(O7C6C5) + δ(O8C5C6)
632	648			δ(O12C11O13) + δ(C9C10C11)
609	603	603	600	γ(O13H21)
567	590			16a + γ(O13H21)
585	576	580	564	6a
534	555			6a + δ(C9C10C11) + δ(C10C11O12)
503	522	534		6a + δ(C3C9C10)
458	459	459	455	γ(O7H18)

[a] ν, stretching; δ, in-plane bending; and γ, out-of-plane bending.

TABLE 4: Calculated (Scaled by 0.972) and Experimental Vibrational Frequencies of Caffeic Acid Complex (Stoichiometry 1:1) and Tentative Assignment According to Wilson's Notation for Benzene Rings[a]

	experimental			
calculated	infrared (solid)	Raman (solid)	Raman (solution)	tentative assignment
1768	1684	1677	1693	ν(C11O12)
1653	1637	1632	1633	ν(C9C10)
1611	1604	1601	1606	8b
1569	1535	1533		8a
1482	1445	1449		19a
1437	1435			19b + ν(C5O8)
1372	1367	1361		δ(C11O13H21) + δ(C9C10H20)
1325	1326	1329		14 + δ(C3C9H19)
1302	1304	1298		14 + δ(C3C9H19)
1263	1280	1280	1287	7a + ν(C5O8) + δ(C11O13H21)
1253				14 + ν(C6O7)
1233	1239			3 + δ(C9C10H20) + δ(C11O13H21) + νs(C6O7,C5O8)
1190	1200	1205	1197	14 + νas(C6O7,C5O8)
1138				18b + ν(C3C9) + νas(C6O7,C5O8)
1127	1120	1121	1119	18a + ν(C3C9) + ν(C11O13) + δ(C11O13H21)
1107	1105	1109		18a + νas(C6O7,C5O8) + ν(C11O13)
1004	977			γ(C9H19) + γ(C10H20)
963	960	961		18b + δ(C3C9C10C11)
937	932			18b + ν(C10C11) + ν(C11C12)
922				17b
864	849	853		11 + γ(C10H20)
855				5 + γ(C10H20)
817	817			12 + νas(O7Al,O8Al)
811	803	799	807	5 + γ(C9C10C11)
774	780	783		12 + δ(C3C9C10)
763				νas(O7Al,O8Al)
747				νs(O7Al,O8Al)
730	739			4 + γ(O13H21)
701	711	714		4 + γ(O13H21) + δ(O7C6C5) + δ(O8C5C6)
634				δ(O12C11O13) + δ(C9C10C11)
624				γ(O13H21)
575	594		596	16a + γ(O13H21)
573	586			6a
525	540		546	6a + δ(C9C10C11) + δ(C10C11O12) + δ(O7AlO8)
504	509			6a + δ(C3C9C10)
450	455	449		δ(O7AlO8)

[a] ν, stretching; δ, in-plane bending; and γ, out-of-plane bending.

that Al(III) does not coordinate with the carboxylate group, because in this case, the coupling of the two C−O stretching modes of the carboxylate group would occur and greatly modify the related frequencies.

The modifications observed between the free and complexed ligands' spectra have, to some extent, essentially two origins: (i) mechanical couplings between vibrators change due to the low, but non-negligible, structural modifications of the ligand engendered by the complexation and (ii) in caffeic acid, the C−O−H in-plane bending modes of hydroxyls of catechol group are largely mixed with ring vibrations; the deprotonation of hydroxyls occurring with chelation eliminates the C−O−H bending and, consequently, modifies both frequencies and couplings of benzene ring modes in complex. The first point could be illustrated, for instance, by the C9−C10 stretching mode. In the free ligand, this mode is low enough in frequency to be coupled with the 8b ring mode, leading to the observation of two bands (at 1645 and 1619 cm^{-1} in the FTIR spectra) corresponding to a mixture of these vibrators. The shortening of the C9−C10 bond length calculated for the complex leads to an increase of the stretching frequency that breaks the mechanical coupling with the 8b mode, and two pure vibrational modes are observed in the complex spectra (at 1637 and 1604 cm^{-1} for the C9−C10 stretching and 8b modes respectively, in the FTIR spectra). Concerning the second point, an example is given by the 8a and 19a modes of the benzene ring. These modes are quasi pure in the complex, whereas they are found mixed with OH bending vibrations of catechol in free caffeic acid. This modification leads to important frequency shifts; the 8a and 19a modes are located at 1601 and 1529 cm^{-1}, respectively, in free molecule FTIR spectra, whereas they are observed at 1535 and 1445 cm^{-1} for the complex. Frequency calculations of free and complexed ligands are in good agreement with these spectral changes.

One other source of spectral modifications lies in the C−O stretching modes of the catechol group. The frequencies and, consequently, the mechanical coupling of these modes are greatly affected by the coordination of Al(III). The 19b mode of caffeic acid, located at 1450 cm^{-1} in the infrared spectrum and calculated pure at 1452 cm^{-1}, is coupled with the C5−O8 stretching in the complex, and its wavenumber shifts to 1435 cm^{-1} (calculated at 1437 cm^{-1}). The appearance of a broad absorbance band centered on 1200 cm^{-1} in the FTIR spectrum of the complex has been assigned to the antisymmetric stretching of C6−O7 and C5−O8 coupled with mode 14. The symmetric and antisymmetric Al−O7 and Al−O8 stretchings have been calculated to be at 747 and 763 cm^{-1}, respectively, but do not give rise to infrared absorption or a Raman diffusion band. All the observations drawn from the spectra assignment clearly confirm the hypothesis that chelation of aluminum ion occurs with the catechol function, which has undergone deprotonation during complexation process.

3.4. Electronic Spectroscopy. The experimental and calculated (vertical lines) electronic spectra of caffeic acid are

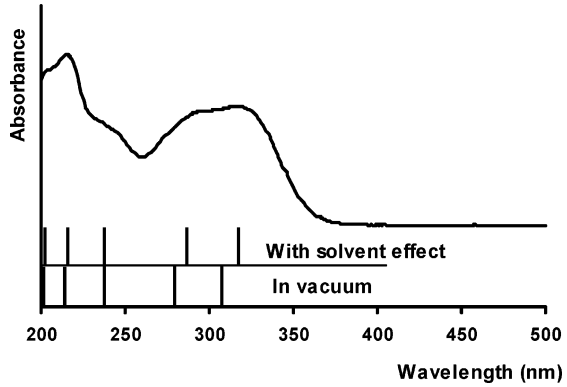

Figure 5. UV−visible spectrum of caffeic acid in methanol and positions of electronic transitions, calculated both in a vacuum and with the solvent effect.

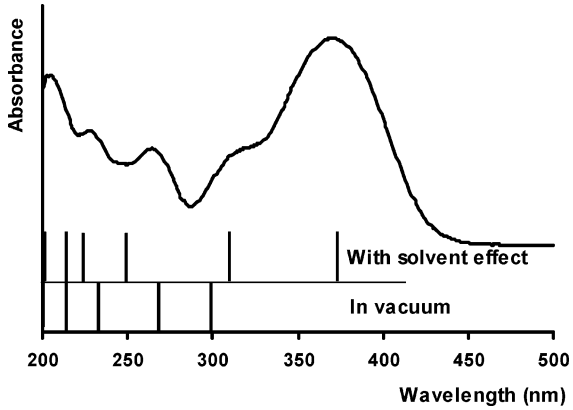

Figure 6. UV−visible spectrum of the 1:1 complex of caffeic acid in methanol and positions of electronic transitions, calculated both in a vacuum and with the solvent effect.

represented in Figure 5. The theoretical spectra have been obtained by a TD-DFT treatment with and without taking into account the solvent effect. The effect of methanol solvation was considered through the self-consistent reaction field method using the SCIPCM model. Table 5 sums up the experimental and calculated wavelengths and computed oscillator strengths both in a vacuum and in methanol. Furthermore, molecular orbitals (with major contributions) involved in each calculated transition in methanol are also reported. The comparison of the major contribution of molecular orbitals involved in each transition has allowed us to determine a correspondence between the calculated wavelengths in a vacuum and in methanol. One can notice that solvent effect becomes non-negligible for the high-wavelength transitions. A very good agreement is observed between the wavelengths of calculated transitions with solvent effect and the UV absorption bands; this demonstrates the validity and accuracy of the method used.

The UV−visible spectrum of the 1:1 complex obtained by singular value decomposition (Specfit) is presented in Figure 6. The theoretical spectra obtained from quantum chemical calculations are represented by vertical lines. In contrast with the calculated spectra of caffeic acid, one can observe a great difference between spectra of the complex calculated in a vacuum and in methanol. In a vacuum, the theoretical spectrum does not reproduce the experimental one, neither in wavelengths, nor in number of observed bands. Moreover, two of the five calculated transitions in a vacuum present relatively low oscillator strengths compared to those obtained when taking into account solvent effect. Except for the transition calculated at 249.8 nm, the positions of theoretical transitions in methanol are in good agreement with the experimental feature. Notably, the position of the two most important bands in the long wavelengths is very well calculated, and the bathochromic shifts obtained by aluminum chelation are reasonably reproduced by calculation. This allows (i) a validation of the spectral decomposition of the mixture of different complexed forms and (ii) a second spectroscopic corroboration of the hypothesis of chelation on the catecholate group.

The molecular orbitals involved in electronic transitions of caffeic acid and of its 1:1 complex are depicted in Figure 7. For caffeic acid, the HOMO essentially has a pronounced π character on the benzene ring, but also implicates nonbonding orbitals of the O atoms of catechol. The first absorption band in the long wavelengths (calculated at 316.3 nm) of the spectrum is primarily due to the HOMO → LUMO transition, which accounts for a contribution of 72%. For this transition, the electronic charge density is withdrawn from the benzene ring

TABLE 5: Experimental and Calculated (in a Vacuum and in Methanol) Absorption Wavelengths[a]

	expt	calculated in vacuum		calculated with solvent effect			
	λ (nm)	λ (nm)	f	λ (nm)	f	M.O.	contribution (%)
free ligand in methanol	314	307.6	0.52	316.3	0.45	HOMO ⇒ LUMO	72
						HOMO−1 ⇒ LUMO	10
	289	277.0	0.14	284.3	0.21	HOMO−1 ⇒ LUMO	75
						HOMO ⇒ LUMO+1	10
	238	236.8	0.07	237.3	0.07	HOMO ⇒ LUMO+1	65
						HOMO−3 ⇒ LUMO	11
	213	216.6	0.13	215.7	0.15	HOMO−3 ⇒ LUMO	67
	202	201.1	0.12	202.8	0.11	HOMO ⇒ LUMO+2	53
						HOMO−1 ⇒ LUMO+1	33
complexed ligand in methanol	370	300.4	0.28	373.1	0.27	HOMO ⇒ LUMO+1	73
						HOMO−1 ⇒ LUMO+1	10
	311	268.9	0.24	306.5	0.34	HOMO−1 ⇒ LUMO+1	77
	263	234.8	0.07	249.8	0.13	HOMO ⇒ LUMO+2	71
						HOMO−2 ⇒ LUMO+1	10
	225	216.4	0.03	220.3	0.15	HOMO−2 ⇒ LUMO+1	70
						HOMO−1 ⇒ LUMO+3	10
	214 (sh)			216.2	0.07	HOMO ⇒ LUMO+3	73
						HOMO−1 ⇒ LUMO+2	13
	203	201.8	0.26	200.1	0.14	HOMO−1 ⇒ LUMO+2	60
						HOMO−6 ⇒ LUMO+1	17

[a] f is relative to the calculated oscillator strengths. The last two columns report the major molecular orbitals and mono-excitation contributions (in %) involved in each calculated transition. (sh = shoulder)

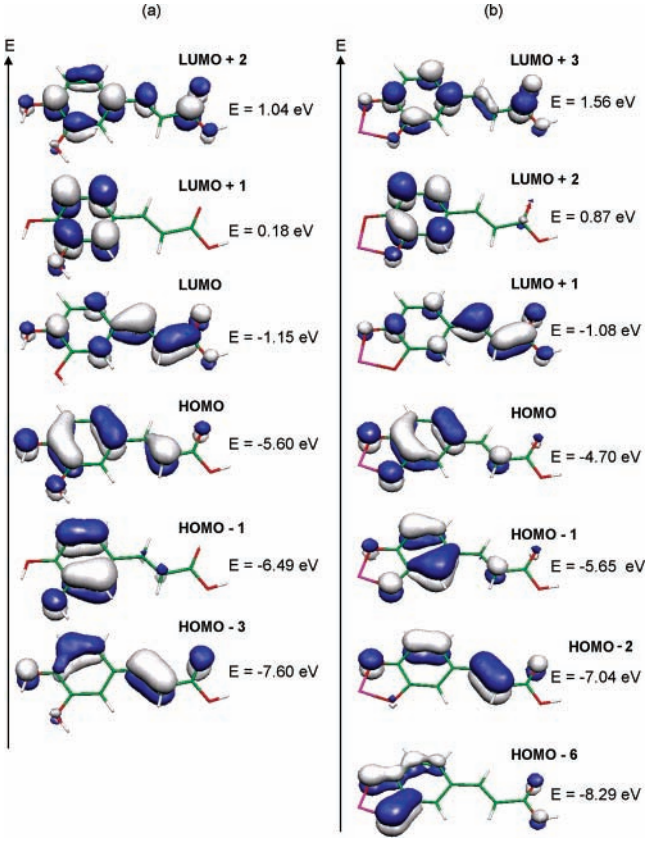

Figure 7. Plots of relevant molecular orbitals involved in the electronic transitions of (a) caffeic acid and (b) its 1:1 complex. The energy of each MO is given in eV.

to the aliphatic chain. HOMO−1 and LUMO+1 are quasi pure orbitals of the benzene ring with bonding and antibonding character, respectively. The charge transfer from the benzene ring to the aliphatic chain is also very pronounced in the HOMO−1 → LUMO transition, which predominantly occurs in the band calculated at 284 nm. The other bands in the short-wavelength range involve orbitals localized over the entire molecule. In the complex, the calculated molecular orbitals present great similarities to those obtained for the free ligand and are presented one-to-one in Figure 7. The LUMO of the complex (not represented in Figure 7b) is fully localized on the aluminum ion and is not implicated in UV−visible transitions. If one considers that LUMO+1 is the lowest unoccupied molecular orbital whose charge density is localized on the ligand, the spectral assignment of the complex is very close to that of caffeic acid. Indeed, from Table 5, one can see that for both free and complexed ligands, the MOs involved in each transition are those that display roughly the same shapes and that have been linked in Figure 7. Notably, the first three transitions at long wavelengths involve exactly the same molecular orbitals, with fairly similar contributions. Thus, the main electronic spectral changes occurring with chelation are essentially due to significant differences in the energies of the MOs.

4. Conclusion

Complexation reactions of potentially toxic metals with naturally occurring organic molecules, such as humic substances, are being recognized as important factors in many natural systems because these reactions determine the speciation and bioavailability of the metal species. The results of this study provide further information regarding the complexation of Al(III) ions with caffeic acid, which can be considered as a model molecule of humic substances. Among the two potential chelating sites in competition within the molecule, we have demonstrated that the catechol group demonstrates the greater complexing power toward Al(III) in methanol solution. The most predominant complexed form obtained for a low amount of aluminum chloride is clearly the 1:1 complex, which is achieved with a complete deprotonation of the catechol function. A large amount of Al(III) is necessary to complex the carboxylate site, and this complexation occurs only after the stronger site is fully occupied. These results allow us to classify the carboxylate function among the different sites already studied: α-hydroxycarbonyl > β-hydroxycarbonyl > catechol > carboxylate.

UV−visible, Raman, and infrared spectroscopies, combined with quantum chemical calculations, have been convenient in establishing the chelating site preferentially involved in caffeic acid. Numerous authors consider that the strongest sites of metal chelation in humic substances are the carboxylic functions with strong acid characteristics and often use simple organic acids as model molecules to interpret or to compare the metal−MO interactions. This work shows that other functions and, notably, the polyphenolic groups are not insignificant in such interactions; they can easily react with Al(III) and modify aluminum speciation.

Acknowledgment. This work is part of the "Programme de Recherche Concertée: Sites et Sols Pollués", supported by the "Région Nord-Pas de Calais" and the "Fonds Européen de Développement Economique des Régions" (FEDER). "Institut du Développement et des Ressources en Informatique Scientique" (IDRIS, Orsay, France) is thankfully acknowledged for the allocation of CPU time. The authors also thank the Lille University Computational Center.

References and Notes

(1) Stevenson, F. J. *Humus Chemistry: Genesis, Composition, Reactions*; Wiley: New York, 1982.
(2) Stevenson, F. J.; Vance, G. F. In *The Environmental Chemistry of Aluminium;* Sposito, G., Ed.; CRC: Boca Raton, 1989; p 145.
(3) Coulson, C. B.; Davies, R. I.; Lewis, D. A. *Soil Sci.* **1960**, *11*, 20.
(4) Remko, M.; Polcin, J. *Collect. Czech. Chem. Commun.* **1980**, *45*, 201.
(5) Smith, D. S.; Kramer, J. R. *Environ. Int.* **1999**, *25*, 295.
(6) Smith, D. S.; Kramer, J. R. *Anal. Chim. Acta* **2000**, *416*, 211.
(7) Boudet, A. C.; Cornard, J. P.; Merlin, J. C. *Spectrochim. Acta* **2000**, *56*, 829.
(8) Cornard, J. P.; Boudet, A. C.; Merlin, J. C. *Spectrochim. Acta* **2001**, *57*, 591.
(9) Cornard, J. P.; Merlin, J. C. *J. Mol. Struct.* **2001**, *569*, 129.
(10) Cornard, J. P.; Merlin, J. C. *J. Inorg. Biochem.* **2002**, *92*, 19.
(11) Cornard, J. P.; Merlin, J. C. *Polyhedron* **2002**, *21*, 2801.
(12) Cornard, J. P.; Merlin, J. C. *J. Mol. Struct.* **2003**, *651*, 381.
(13) Olsen, R. A.; Brown, J. C.; Bennet, J. H.; Blume, D. *J. Plant. Nutr.* **1982**, *5*, 433.
(14) Yoe, J. H.; Jones, L. *Ind. Eng. Chem., Anal. Ed.* **1944**, *16*, 11.
(15) Specfit Global Analysis System, Spectrum Software Associates, Marlborough, MA.
(16) Gampp, H.; Maeder, M.; Meyer, C. J.; Zuberbühler, A. *Talanta* **1986**, *33*, 943.
(17) Frisch, M. J.; Trucks, G. W.; Schlegel, H. B.; Scuseria, G. E.; Robb, M. A.; Cheeseman, J. R.; Zakrzewski, V. G.; Montgomery, J. A., Jr.; Stratmann, R. E.; Burant, J. C.; Dapprich, S.; Millam, J. M.; Daniels, A. D.; Kudin, K. N.; Strain, M. C.; Farkas, O.; Tomasi, J.; Barone, V.; Cossi, M.; Cammi, R.; Mennucci, B.; Pomelli, C.; Adamo, C.; Clifford, S.; Ochterski, J.; Petersson, G. A.; Ayala, P. Y.; Cui, Q.; Morokuma, K.; Malick, D. K.; Rabuck, A. D.; Raghavachari, K.; Foresman, J. B.; Cioslowski, J.; Ortiz, J. V.; Baboul, A. G.; Stefanov, B. B.; Liu, G.; Liashenko, A.; Piskorz, P.; Komaromi, I.; Gomperts, R.; Martin, R. L.; Fox, D. J.; Keith, T.; Al-Laham, M. A.; Peng, C. Y.; Nanayakkara, A.; Challacombe, M.; Gill, P. M. W.; Johnson, B.; Chen, W.; Wong, M. W.; Andres, J. L.; Gonzalez, C.; Head-Gordon, M.; Replogle, E. S.; Pople, J. A. *Gaussian 98*, revision A.9; Gaussian, Inc.: Pittsburgh, PA, 1998.
(18) Becke, A. D. *J. Chem. Phys.* **1993**, *98*, 5648.

(19) Lee, C.; Yang, W.; Parr, R. G. *Phys. Rev. B: Condens. Matter Mater. Phys.* **1988**, *37*, 785.
(20) Scott, A. P.; Radom, L. *J. Phys. Chem.* **1996**, *100*, 16513.
(21) Dupuis, M.; Marquez, A.; Davidson, E. R. "*HONDO 95.3 from CHEM-Station*" 1995, IBM Corporation, Neighborhood Road, Kingston, NY 12401.
(22) Bauernschmitt, R.; Ahlrichs, R. *Chem. Phys.* **1996**, *256*, 454.
(23) Foresman, J. B.; Keith, T. A.; Wiberg, K. B.; Snoonian, J.; Frisch, M. J. *J. Phys. Chem.* **1996**, *100*, 16098.
(24) Sikora, F. J.; McBride, M. B. *Soil Sci. Soc. Am. J.* **1990**, *54*, 78.
(25) Adams, M. L.; O'Sullivan, B.; Downard, A. J.; Powell, K. J. *J. Chem. Eng. Data* **2002**, *47*, 289.
(26) Motekaitis, R. J.; Martell, A. E.; *Inorg. Chem.* **1984**, *23*, 18.
(27) Downard, A. J.; O'Sullivan, B.; Powell, K. J. *Polyhedron* **1996**, *15*, 3469.
(28) Ohman, L. O.; Sjoberg, S. *Polyhedron*, **1983**, *12*, 1329.
(29) Sikora, F. J.; McBride, M. B. *Environ. Sci. Technol.* **1989**, *23*, 349.
(30) Porter, L. J.; Markham, K. R. *J. Chem. Soc. Perkin Trans. 1* **1970**, *9*, 1309.
(31) Porter, L. J.; Markham, K. R. *Phytochemistry* **1972**, *11*, 1477.
(32) Kiss, T.; Nagy, G.; Pecsi, M. *Polyhedron* **1989**, *8*, 2345.
(33) Linder, P. W.; Voyé, A. *Polyhedron* **1987**, *6*, 53.
(34) Petrou, A. L.; Koromantzou, M. V.; Tsangaris, J. M. *Chim. Chron.* **1993**, *22*, 189.
(35) VanBesien, E.; Marques, M. P. M. *THEOCHEM* **2003**, *625*, 265.
(36) Tannor, D. J.; Marten, B.; Murphy, R.; Friesner, R. A.; Sitkoff, D.; Nicholls, A.; Ringnalda, M.;. Goddard, W. A.; Honig, B. *J. Am. Chem. Soc.* **1994**, *116*, 11875.
(37) Marten, B.; Kim, K.; Cortis, C.; Friesner, R. A.; Murphy, R. B.; Ringnalda, M. N.; Sitkoff, D.; Honig, B. *J. Phys. Chem.* **1996**, *100*, 11775.
(38) Jaguar 4.2, Schrödinger, L.L.C., Portland, OR, 1991−2002.
(39) Sanchez-Cortés, S.; Garcia-Ramos, J. V. *Spectrochim. Acta* **1999**, *55*, 2935.
(40) Sanchez-Cortés, S.; Garcia-Ramos, J. V. *Appl. Spectrosc.* **2000**, *54*, 230
(41) Sanchez-Cortés, S.; Francioso, O.; Garcia-Ramos, J. V.; Ciavatta, C.; Gessa, C. *Colloids Surf., A* **2001**, *176*, 177.
(42) Varsanyi, G. In *Assignment for Vibrational Spectra of 700 Benzene Derivates*; Lang, L, Ed.; Hilger: Budapest, 1974.
(43) Williams, P. A. M.; Baro, A. C. G.; Ferrer, E. G. *Polyhedron* **2002**, *21*, 1979.